

ASME Journal of Biomechanical Engineering Online journal at:

https://asmedigitalcollection.asme.org/biomechanical



Eden Winslow

Department of Biomedical Engineering, University of California Davis, Davis, CA 95616

Xuanbei Pan

Department of Biomedical Engineering, University of California Davis, Davis, CA 95616

Maury L. Hull

Department of Biomedical Engineering,
University of California Davis,
Davis, CA 95616;
Department of Mechanical Engineering,
University of California Davis,
Davis, CA 95616;
Department of Orthopaedic Surgery,
University of California Davis,
Davis, CA 95616

Analysis of Variation in Sagittal Curvature of the Femoral Condyles

In designing femoral components, which restore native (i.e., healthy) knee kinematics, the flexion–extension (F-E) axis of the tibiofemoral joint should match that of the native knee. Because the F-E axis is governed by the curvature of the femoral condyles in the sagittal plane, the primary objective was to determine the variation in radii of curvature. Eleven high accuracy three-dimensional (3D) femur models were generated from ultrahigh resolution CT scans. The sagittal profile of each condyle was created. The radii of curvature at 15 deg increments of arc length were determined based on segment circles best-fit to ± 15 deg of arc at each increment. Results were standardized to the radius of the best-fit overall circle to 15 deg-105 deg for the femoral condyle having a radius closest to the mean radius. Medial and lateral femoral condyles exhibited multiradius of curvature sagittal profiles where the radius decreased at 30 deg flexion by 10 mm and at 15 deg flexion by 8 mm, respectively. On either side of the decrease, radii of segment circles were relatively constant. Beyond the transition angles where the radii decreased, the anterior-posterior (A-P) positions of the centers of curvature varied 4.8 mm and 2.3 mm for the medial and lateral condyles, respectively. A two-radius of curvature profile approximates the radii of curvature of both native femoral condyles, but the transition angles differ with the transition angle of the medial femoral condyle occurring about 15 deg later in flexion. Owing to variation in A-P positions of centers of curvature, the F-E axis is not strictly fixed in the femur. [DOI: 10.1115/1.4065813]

Keywords: total knee replacement, total knee arthroplasty, flexion-extension axis, prosthetic, femoral component, femoral implant

Introduction

One of the major goals of total knee arthroplasty (TKA) is to restore native (i.e., healthy) knee kinematics. To do so entirely would require that the three kinematic axes of the prosthetic joint replicate those of the native knee [1,2]. Restricting attention to the primary axis, which is the flexion–extension (F-E) axis of the tibiofemoral joint, ideally the curvature of the prosthetic femoral condyles in the sagittal plane would match the curvature of the native femoral condyles. Accordingly, information important to the design of prosthetic femoral components is the radii of curvature of the medial and lateral femoral condyles and any variations in the radii with flexion.

Recognizing the need for the information above, the curvature of the native femoral condyles in the sagittal plane has been studied using different methods. One method fit various mathematical functions particularly to the posterior femoral condyles [3,4], another method used B-splines [5], a third method fit two circular arcs [6], and a fourth method used best-fit single circles [7–11]. Of these methods, only the use of B-splines fit to segments of arc length was able to illustrate local variations in radius of curvature. The

Manuscript received January 20, 2024; final manuscript received June 5, 2024; published online July 16, 2024. Assoc. Editor: Bruce MacWilliams.

main finding was that the radii of curvature of the condyles showed a standard deviation of 2.4 mm laterally and 2.2 mm medially on average so that the condyles are not circular. However, a limitation was that results were not standardized thus introducing inflated variability.

Perhaps because of the different methods used to study the radius of curvature and the lack of consistency in results (i.e., constant versus variable curvature), there is a distinct lack of consensus among manufacturers regarding the curvature of the femoral condyles as evidenced by design variations in prosthetic femoral components in the commercial marketplace. At least three fundamentally different designs can be identified. These include constant radius [12,13], multiradius, which is the most common [12,14], and gradually reducing radius designs [15]. Regarding multiradius designs, design details such as the transition angle(s) (i.e., flexion angle(s) where the radius of curvature decreases), the magnitude of decrease in radius of curvature, and the number of decreases vary between manufacturers [12,15]. Given this lack of consensus and the limitation concerning inflated variability in the study by Kosel et al. [5] noted above, additional morphological information regarding the sagittal curvature of the femoral condyles, which governs the F-E axis, is warranted.

The primary objectives of this study were twofold. Using highly accurate three-dimensional (3D) femur models, one objective was to

determine whether the curvature of the medial and lateral femoral condyles in the sagittal plane varies with flexion. A related objective was to determine the variation in the locations of the centers of curvature, which is relevant to assessing whether the F-E axis is fixed in the femur.

Materials and Methods

Because the materials and methods to create the 3D femur models have been described previously [16], description will be limited to aspects that are important to the study herein. Eleven fresh-frozen human cadaveric lower limb specimens (mean age: 81 ± 10.3 , range 60-98 years, 7 females, 4 males) were included in the study. Refer to the Appendix for measurements of morphological variables (Table 1). Since the study used de-identified cadaveric specimens, institutional review board approval at the University of California Davis was unnecessary. Radiographic screening showed that each specimen was free of bone abnormalities and arthritis of the knee. Each specimen was scanned on an ultrahigh resolution CT system (Aquilion Precision, Canon Medical Systems, Otawara, Japan) [16]. Specimens were scanned in high-resolution mode with a slice thickness of 0.5 mm. Consistent with results from the radiographic screening, high resolution images confirmed the absence of bone abnormalities (e.g., osteophytes) and arthritis of the knee. Using the automatic tools in conjunction with manual refinement, software was used to segment bone surfaces depicted on the CT images (MIMICS® v20.0, Materialize, Belgium). 3D models of femurs were constructed using the "marching cubes algorithm."

Each model was imported into Geomagic (CONTROL X 2022, Oqton, Los Angeles, CA) where it was oriented in the kinematic planes. The coronal plane was defined as simultaneously tangent to the most posterior points of both condyles and the most posterior point of the greater trochanter. With the posterior condyles superimposed, the sagittal plane was perpendicular to the coronal plane, and the transverse plane was therefore mutually perpendicular to these two.

The defeature tool in Geomagic was used to smooth any artifacts on the surface of the condyles (Defeature Type: fill, Method: curvature, Smooth Boundary of Defeatured Area: yes). The tool performs by deleting the chosen portion of the model and then filling it in tangent to the surrounding curvature of the surface. It was used only in a localized manner around obvious artifacts, and the compare tool in Geomagic was utilized to assess the model before and after smoothing to ensure that there was no change in the macroscopic curvature of the condyles. The compare tool evaluated the shortest distance between equivalent points in the model; most differences were < 0.2 mm, with the maximum difference < 0.5 mm and localized to individual artifacts.

After converting the model file to a type that could be analyzed in MATLAB, a local coordinate system was created for each condyle. Using the sagittal profile defined as the projection in the sagittal plane, a best-fit overall circle was applied to the profile of each condyle from 15 deg to 105 deg, a range of flexion approximately circular [7–11]. The best-fit overall circle was calculated using the CircleFitbyPratt function, which minimizes the sum of squared radial deviations and returns the origin and radius of the circle [17]. The origin was the center of the circle (Fig. 1). The x-axis was positive to the left side of the body, the y-axis was positive posteriorly, and the z-axis was positive proximally. The negative z-axis defined the 0 deg flexion reference.

Following this, radii of curvature of arc segments along the sagittal profile were found as a function of flexion angle from 0 deg to 120 deg. The condyle was segmented by center angles in 15 deg increments relative to the 0 deg flexion angle reference and included 15 deg of arc on either side of the center angle. The first segment at 0 deg only used the positive 15 deg arc because the negative portion extended beyond the curvature of the condyle involved in flexion. Again, using the CircleFitbyPratt function, a circle was best fit to each arc segment to determine the radius of curvature for that arc segment. Two best-fit segment circles had to be excluded due to the function incorrectly fitting a circle with inverse curvature. Other analytical metrics calculated included the root-mean-square (RMS)

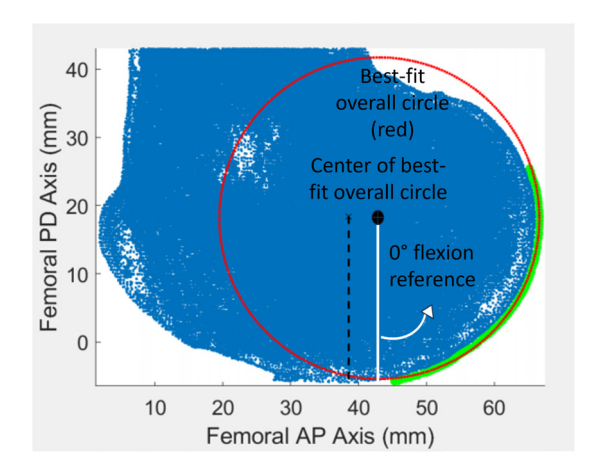


Fig. 1 Example best-fit overall circle (red line) to the sagittal profile (green line) of the medial femoral condyle for a specimen. The horizontal and vertical axes labels are the femoral anterior-posterior (AP) axis the the femoral proximal-distal (PD) axis, respectively. The 0 deg flexion reference was a line parallel to the coronal plane (dashed line) and positioned at the center of the best-fit overall circle.

radial deviation and the RMS radial deviation normalized to the radius of the best-fit segment circle (termed the relative RMS radial deviation), which describes the quality of the fit for each arc segment.

Statistical Analysis. To determine whether the radii of curvature varied with flexion angle, the medial and lateral radii were standardized. To do this, means and standard deviations of best-fit overall circles were calculated for each condyle. The radius of the best-fit overall circle closest to the mean for a particular condyle was chosen as the standard. The scaling factor was calculated by dividing the standard femur's best-fit overall circle radius by the best-fit overall circle radius for each of the other femurs. Once the scaling factor for a particular femur was determined, the best-fit segment circle radii for each femur were multiplied by their respective scaling factors. Following standardization, means and standard deviations were calculated for best-fit segment circles. Ninety five percent confidence limits were placed on the means.

To determine whether the radii of curvature differed between lateral and medial condyles, the radii of the best-fit overall circles (nonstandardized) were compared using a paired t-test. For this test, a power analysis confirmed that with 11 femurs, differences in condyle radii with an effect size of 0.8, could be detected with $\alpha = 0.05$ and $(1-\beta) \ge 0.80$. With a standard deviation of 2.6 mm, the difference to detect was 2 mm. To determine the variation in sizes, the range of the radii from the best-fit overall circles was found.

Results

Both the medial and lateral femoral condyles exhibited multiradius of curvature sagittal profiles, but the transition angles differed (Fig. 2). For the medial femoral condyle, the mean standardized radius of curvature of segment circles was relatively constant at about 32 mm to 30 deg of flexion, decreased notably by about 10 mm at 45 deg of flexion, and was relatively constant for the remainder of flexion. In contrast, for the lateral femoral condyle, the mean standardized radius of curvature of segment circles was about 30 mm at 15 deg of flexion but decreased notably by about 8 mm at 30 deg of flexion and was relatively constant after. Although the transition angles differed, the standardized radii of segment circles before and after the transitions were approximately equal.

Because the standardized radii of curvature of segment circles varied with flexion for each femoral condyle, locations of the corresponding standardized centers of curvature varied somewhat as well (Fig. 3). For each condyle, variation in locations of

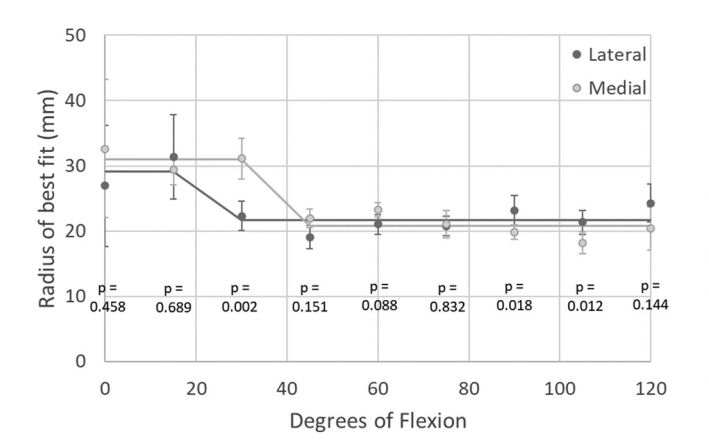


Fig. 2 Mean and 95% confidence intervals of the standardized radii of best-fit segment circles at 15 deg increments of arc length along the sagittal profiles of the 3D femur models for the medial and lateral femoral condyles. Horizontal lines indicate means over the flexion angle range spanned by each line.

approximately 5 mm around the origin of the best-fit overall circle used for standardization was greatest before the transition angle where the standardized radii of curvature of segment circles were largest (Fig. 2). After the transition angle, variation in locations was notably less reflecting the relatively constant standardized radii of curvature of segment circles (Fig. 2).

The quality of the best-fit segment circles was comparable between the medial and lateral femoral condyles. For the lateral femoral condyle, the mean RMS radial deviation within a flexion angle ranged from $3.4\times10^{-2}\,\mathrm{mm}$ to $6.0\times10^{-2}\,\mathrm{mm}$ and the mean relative RMS radial deviation ranged from $1.5\times10^{-3}\,\mathrm{mm}$ to $2.6\times10^{-3}\,\mathrm{mm}$. For the medial femoral condyle, the mean RMS radial deviation within a flexion angle ranged from $3.5\times10^{-2}\,\mathrm{mm}$ to $5.8\times10^{-2}\,\mathrm{mm}$ and the mean relative RMS radial deviation ranged from $1.2\times10^{-3}\,\mathrm{mm}$ to $2.8\times10^{-3}\,\mathrm{mm}$.

The radii of curvature of the best-fit overall circles from 15 deg to 105 deg differed significantly between the medial and lateral

Mean Medial Centers of Curvature

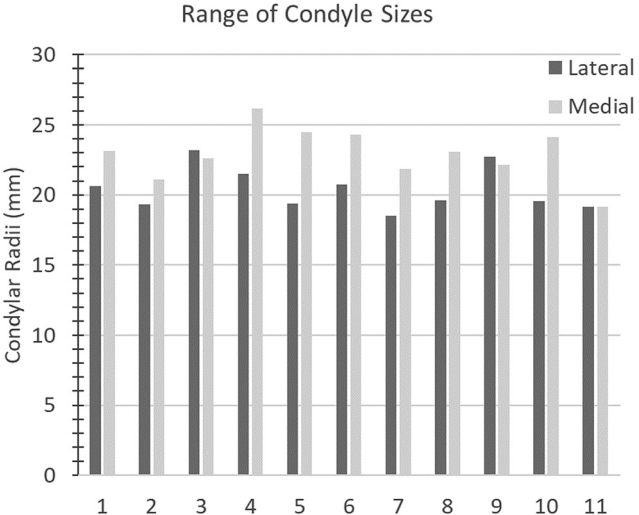


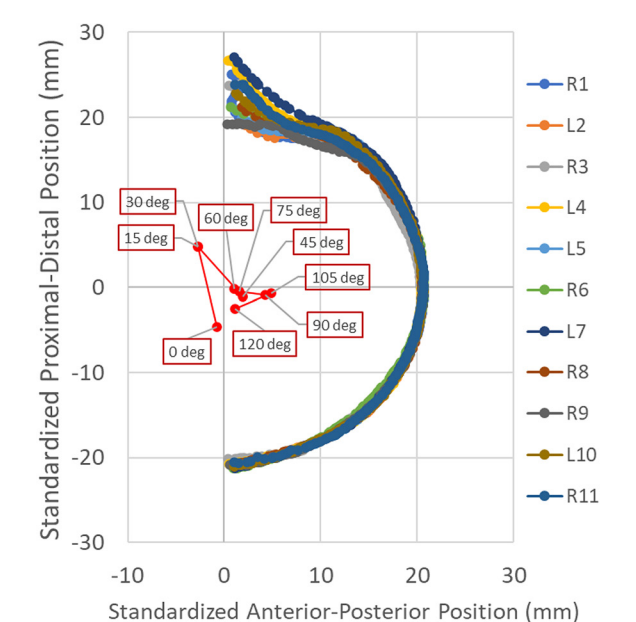
Fig. 4 Column graph illustrating the radii of the medial and lateral femoral condyles for the best-fit overall circles over the flexion range 15 deg-105 deg for each of the 11 femur models

femoral condyles. The radius of the medial femoral condyle was notably greater in 8 of the 11 femur-cartilage models and within 0.5 mm or less for the remaining 3 models (Fig. 4). Hence, the mean radius of the medial femoral condyle was 2.5 mm greater than the lateral (p = 0.0026).

The radii of curvature of the best-fit overall circles exhibited a wide range (Fig. 4). The range for the lateral femoral condyle was 18.5 mm to 23 mm, whereas the range for the medial femoral condyle was 19 mm to 26 mm.

Discussion

The most important findings of this study were that (1) both the medial and lateral femoral condyles exhibited multiradius of curvature sagittal profiles with differing transition angles,



Mean Lateral Centers of Curvature

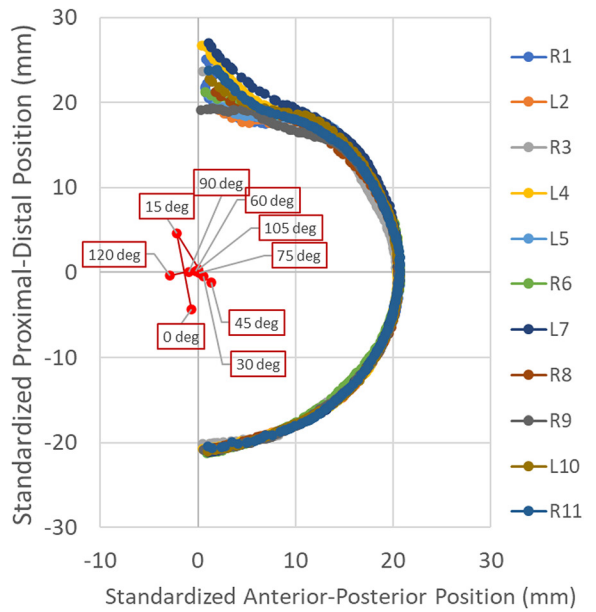


Fig. 3 Plots of the mean centers of curvature (red dots) for the standardized radii of best-fit segment circles for the medial and lateral femoral condyles and standardized sagittal profiles for each 3D femur model

(2) locations of the centers of curvature for the standardized best-fit segment circles varied for both femoral condyles, (3) the radius of the best-fit overall circle was significantly greater for the medial than the lateral femoral condyle, and (4) the radii of the best-fit overall circles exhibited a wide range.

Since the mean radius of the best-fit overall circle was greater for the medial than the lateral femoral condyle by 2.5 mm, it might be tempting to conclude that this difference should be reflected in femoral component design. However, because the best-fit overall circle spanned the flexion range of 15 deg—105 deg and because the standardized radius of curvature of the best-fit segment circle at 30 deg flexion was significantly greater for the medial condyle than the lateral condyle (Fig. 2), the radius of the best-fit overall circle was somewhat inflated by this difference. Accordingly, rather than the radius of curvature, attention should focus on the difference in transition angles between the condyles.

Both condyles showed larger radii of curvature near extension with the result that a transition angle occurred early in flexion. However, the transition angles differed with that of the lateral condyle occurring 15 deg earlier than the medial condyle. Since the radii of curvature of segment circles were relatively constant before and after the transition angles (Fig. 2), this result suggests that a multiradius femoral component design consisting of two radii approximates the sagittal surfaces of both femoral condyles.

The above finding is consistent with that of a previous study [6]. These authors also reported that a model consisting of two circular arcs closely represented the sagittal profiles of the condyles with transition angles of 39 deg and 18 deg for the medial and lateral condyles, respectively. These angles compare favorably to those in our study where transition angles occurred between 30 deg and 45 deg for the medial condyle and between 15 deg and 30 deg for the lateral condyle (Fig. 2). This close agreement in findings can be traced to the similarity in defining the sagittal plane as the plane perpendicular to the posterior condylar axis.

Our findings also agree with those of another previous study [5]. Using b-splines to approximate the curvature locally, these authors reported for the posterior portions of the condyles that the mean radii were 20.3 mm for the lateral side and 18.7 mm for the medial side and that the curvature was relatively consistent for the posterior condylar surfaces. Past the transition angles, our mean standardized radii of curvature for the best-fit segment circles were 21.4 mm and 20.4 mm for the lateral and medial condyles, respectively, and the radii were relatively constant (Fig. 2).

Since the motivation for our study was to provide information applicable to femoral component design, it is of interest to compare specifics of some commercially available designs to our findings. One previous paper analyzed the variation in curvature for the Medacta GMK sphere and the Persona [12]. Since the Medacta GMK sphere is a single-radius design, the transition angle was necessarily absent. However, the Persona (for size 7) exhibited a transition angle between 45 deg and 60 deg flexion and this angle was the same for both condyles. This transition angle is about 15 deg later in flexion for the medial femoral condyle and some 30 deg later in flexion for the lateral femoral condyle. Since the transition angle in the native knee manifested because the condyles have less curvature near extension, the relatively late transition angle for the Persona does not reflect the geometry of the native knee.

Although the native knee clearly exhibits an abrupt transition angle with relatively constant curvature before and after the angle, the two-radius design with an abrupt transition has been criticized as possibly contributing to midflexion instability where the femur suddenly shifts anterior on the tibia during flexion [15]. A computational study demonstrated that a gradually reducing radius design used with mechanical alignment (MA) limited the instability. This result was confirmed in testing of cadaveric knees. However, this instability has not been observed using unrestricted kinematic alignment (KA) with a two-radius design [18,19]. Hence, midflexion instability may be a phenomenon generic to MA since MA fails to restore native knee function as indicated by abnormal kinematics and high tibial contact forces even after collateral ligament release to

"balance" the knee [20]. In contrast, unrestricted KA, which simply resurfaces the knee thus involving no collateral ligament release, consistently restores these biomechanical metrics closely to native [18,21,22].

Since the mean radii of curvature of standardized best-fit segment circles differed before and after the transition angle with differences approaching 10 mm for both condyles (Fig. 2), the question arises as to whether the F-E axis is indeed fixed in the femur as reported by several studies [9,23–25]. However, since the curvature of the condyles near extension is flatter than that of the posterior condyles, answering this question should focus on the curvature after the transition angle. Variations in the mean centers of curvature were primarily in the anterior-posterior direction (Fig. 3) and ranged over 4.8 mm and 2.3 mm for the medial and lateral condyles, respectively. Hence, the F-E axis varies somewhat, and this variation evidently could not be detected in the methods used by the studies cited above. Because the F-E axis varies somewhat, a two-radius design is an approximation albeit close.

Although a two-radius design might be optimal for restoring the F-E axis of the prosthetic closely to native, TKA implants must be viewed as a system where other considerations come into play to retore native knee function and particularly restoration of the internal-external (I-E) axis. Like the F-E axis, this axis is relatively fixed in the bone but passes approximately parallel to the tibial mechanical axis and through the center of medial articular surface [25,26]. A tibial insert design, which mimics the conformity and soft tissue constraints of the native knee, has a highly conforming (i.e., ball-in-socket) medial articular surface and a flat lateral articular surface, which allows relatively unconstrained A-P movement of the lateral femoral condyle. When used with a femoral component with spherical femoral condyles (i.e., constant radius), this insert design restores the I-E axis and promotes internal tibial rotation particularly when the posterior cruciate ligament is retained [27–30]. However, ball-in-socket medial conformity would not be possible with a tworadius medial femoral condyle. Hence, the designer of TKA implants must weigh the tradeoffs in restoring the F-E axis versus

A unique aspect of our study was the quantitative evaluation of the quality of best-fit segment circles using the RMS radial deviations and the relative RMS radial deviations. The worst-case RMS radial deviations of 0.06 mm were the same for both condyles as were worst-case relative RMS radial deviations which were less than 0.003 (i.e., 0.3%). With these small deviations, it can be concluded that using best-fit segment circles to determine the variation in radius of curvature was a simple yet effective method.

Two aspects of the methodology have the potential to affect our results. One is the method to define the 0 deg flexion reference. To define this reference, the coronal plane was formed and the reference was a line parallel to this plane with the origin centered in the best-fit overall circle (Fig. 1). Hence, results along the flexion arc would be affected by the position of the origin and the line used to define the reference. However, multiple studies have shown that the F-E axis is well defined by the centers of best-fit overall circles [9,23–26,31] so that the centers of these circles are appropriate for determining the flexion angle.

Regarding the 0 deg flexion reference, other common reference lines are the projections of the femoral mechanical and anatomic axes into the sagittal plane. The angular differences between our reference line and these other two reference lines were checked. The greatest differences were 1.6 deg and 1.2 deg for the mechanical and anatomic axes, respectively. Hence, our results would not be markedly impacted by using either of the other two reference lines.

The other aspect of the methodology that could affect our results is the method to define the sagittal plane used for curvature analysis. The same body of literature that supports using the origin of the best-fit overall circle also supports using a sagittal plane where the posterior condyles are superimposed since the F-E axis is perpendicular to this plane. Although using a different sagittal plane could affect results, a different plane would lead to erroneous results. This is because the flexion–extension motion of the

tibiofemoral joint is governed by the curvature of the femoral condyles in the sagittal plane perpendicular to the F-E axis.

One limitation to our study concerns the relatively small sample size. However, the advantage in using these femur models was that generating the models from ultrahigh resolution CT images [16] yielded arguably the most accurate models possible with current CT technology. Since variations in the radii of curvature of the sagittal profiles were of interest, this accuracy was necessary to generate reliable results. A disadvantage was that the models may not fully represent the variation in size so that analysis of a greater number of models likely would result in wider ranges of sizes for the condyles.

A second limitation concerns the use of 3D models developed from CT scans, which did not include articular cartilage. With the absence of articular cartilage, the radii of curvature would have been larger had the articular cartilage been included. Considering that the mean cartilage thickness on the femoral condyles is 2.5 mm in the central region and is relatively consistent within 0.3 mm over the range of flexion [32], the mean radii would have increased by this amount. Although the mean values in Fig. 2 would increase, this increase would not impact our key findings since the increase is systematic.

Conclusion

Our results add new information regarding the sagittal curvature of the native femoral condyles, which can be used to guide the design of femoral components used in TKA. Using highly accurate 3D femur models, our results showed larger radii of curvature near extension and hence the presence of transition angles for both femoral condyles. However, on either side of the transition angles, the sagittal profiles can be approximated with a single radius of curvature. Although a two-radius femoral component design represents the curvature of native femoral condyles, the tradeoffs in restoring the F-E axis versus the I-E axis should be considered when designing a TKA implant system. Owing to variation particularly in the A-P positions of the centers of curvature, the F-E axis is not strictly fixed in the femur.

Acknowledgment

The senior author (MLH) is grateful to Medacta USA, Inc. for financial support of his research program advancing the science and clinical practice of total knee replacement surgery. We thank the individuals who donated their remains and tissues for the advancement of education and research.

Funding Data

- NIAMS funded training program in Musculoskeletal Health Research (No. T32 AR079099).
- NSF NRT (Award No. 2152260).

Data Availability Statement

The datasets generated and supporting the findings of this article are obtainable from the corresponding author upon reasonable request.

Appendix

References

- [1] Howell, S. M., Kuznik, K., Hull, M. L., and Siston, R. A., 2008, "Results of an Initial Experience With Custom-Fit Positioning Total Knee Arthroplasty in a Series of 48 Patients," Orthopedics, 31(9), pp. 857–863.
- [2] Eckhoff, D., Hogan, C., DiMatteo, L., Robinson, M., and Bach, J., 2007, "Difference Between the Epicondylar and Cylindrical Axis of the Knee," Clin. Orthop. Relat. Res., 461, pp. 238–244.
- [3] Rehder, U., 1983, "Morphometrical Studies on the Symmetry of the Human Knee Joint: Femoral Condyles," J Biomech., 16(5), pp. 351–361.
- [4] Rostlund, T., Carlsson, L., Albrektsson, B., and Albrektsson, T., 1989, "Morphometrical Studies of Human Femoral Condyles," J. Biomed. Eng., 11(6), pp. 442–448.
- [5] Kosel, J., Giouroudi, I., Scheffer, C., Dillon, E., and Erasmus, P., 2010, "Anatomical Study of the Radius and Center of Curvature of the Distal Femoral Condyle," ASME J. Biomech. Eng., 132(9), p. 091002.
- [6] Nuño, N., and Ahmed, A. M., 2001, "Sagittal Profile of the Femoral Condyles and Its Application to Femorotibial Contact Analysis," ASME J. Biomech. Eng., 123(1), pp. 18–26.
- [7] Asano, T., Akagi, M., Tanaka, K., Tamura, J., and Nakamura, T., 2001, "In Vivo Three-Dimensional Knee Kinematics Using a Biplanar Image-Matching Technique," Clin. Orthop. Relat. Res., 388, pp. 157–166.
- [8] Elias, S. G., Freeman, M. A., and Gokcay, E. I., 1990, "A Correlative Study of the Geometry and Anatomy of the Distal Femur," Clin. Orthop. Relat. Res., 260, pp. 98–103.
- [9] Hollister, A. M., Jatana, S., Singh, A. K., Sullivan, W. W., and Lupichuk, A. G., 1993, "The Axes of Rotation of the Knee," Clin. Orthop. Relat. Res., 290, pp. 259–268.
- [10] Howell, S. M., Howell, S. J., and Hull, M. L., 2010, "Assessment of the Radii of the Medial and Lateral Femoral Condyles in Varus and Valgus Knees With Osteoarthritis," J. Bone Jt. Surg Am., 92(1), pp. 98–104.
- [11] Pinskerova, V., Nemec, K., and Landor, I., 2014, "Gender Differences in the Morphology of the Trochlea and the Distal Femur," Knee Surg. Sports Traumatol. Arthrosc., 22(10), pp. 2342–2349.
- [12] Hull, M. L., 2022, "Errors in Using Fixed Flexion Facet Centers to Determine Tibiofemoral Kinematics Increase Fourfold for Multi-Radius Femoral Component Designs With Early Versus Late Decreases in the Radius of Curvature," Knee, 35, pp. 183–191.
- [13] Shimizu, N., Tomita, T., Yamazaki, T., Yoshikawa, H., and Sugamoto, K., 2014, "In Vivo Movement of Femoral Flexion Axis of a Single-Radius Total Knee Arthroplasty," J. Arthroplasty, 29(12), pp. 2407–2411.
- [14] Ng, J. W. G., Bloch, B. V., and James, P. J., 2019, "Sagittal Radius of Curvature, Trochlea Design and Ultracongruent Insert in Total Knee Arthroplasty," EFORT Open Rev., 4(8), pp. 519–524.
- [15] Clary, C. W., Fitzpatrick, C. K., Maletsky, L. P., and Rullkoetter, P. J., 2013, "The Influence of Total Knee Arthroplasty Geometry on Mid-Flexion Stability: An Experimental and Finite Element Study," J. Biomech., 46(7), pp. 1351–1357.
- [16] Nedopil, A. J., Rego, E., Hernandez, A. M., Boone, J. M., Howell, S. M., and Hull, M. L., 2024, "Correcting for Asymmetry of the Proximal Tibial Epiphysis is Warranted to Determine Postoperative Alignment Deviations in Kinematic Alignment From Planned Alignment of the Tibial Component on the Native Tibia," Clin. Biomech., 113, p. 106215.
- [17] Chernov, N., 2023, "Circle Fit (Pratt Method)," MATLAB Central File Exchange, accessed July 3, 2024, https://www.mathworks.com/matlabcentral/fileexchange/ 22643-circle-fit-pratt-method
- [18] Nicolet-Petersen, S., Saiz, A., Shelton, T., Howell, S. M., and Hull, M. L., 2020, "Small Differences in Tibial Contact Locations Following Kinematically Aligned TKA From the Native Contralateral Knee," Knee Surg. Sports Traumatol. Arthrosc., 28(9), pp. 2893–2904.
- [19] Delman, C. M., Ridenour, D., Howell, S. M., and Hull, M. L., 2023, "The Posterolateral Upslope of a Low-Conforming Insert Blocks the Medial Pivot During a Deep Knee Bend in TKA: A Comparative Analysis of Two Implants With Different Insert Conformities," Knee Surg. Sports Traumatol. Arthrosc., 31(9), pp. 3627–3636.
- [20] Meneghini, R. M., Ziemba-Davis, M. M., Lovro, L. R., Ireland, P. H., and Damer, B. M., 2016, "Can Intraoperative Sensors Determine the "Target" Ligament Balance? Early Outcomes in Total Knee Arthroplasty," J Arthroplasty, 31(10), pp. 2181–2187.
- [21] Roth, J. D., Howell, S. M., and Hull, M. L., 2018, "Kinematically Aligned Total Knee Arthroplasty Limits High Tibial Forces, Differences in Tibial Forces Between Compartments, and Abnormal Tibial Contact Kinematics During Passive Flexion," Knee Surg. Sports Traumatol. Arthrosc., 26(6), pp. 1589–1601.

Table 1 Mean, standard deviation, and range of morphological variables for males and females

	Femur length (mm)	Epicondylar width (mm)	Transcondylar width (mm)	Lateral AP depth (mm)	Medial AP depth (mm)	Lateral best-fit overall circle (mm)	Medial best-fit overall circle (mm)
Males $(n=4)$	478.3±18.6 (467–506)	85.2±2.8 (82–88)	80.2±0.8 (79–81)	68.3±1.9 (66–70)	66.2±3.8 (61–70)	22.0 ± 1.0 $(20.8-23.2)$	23.8±1.6 (22.1–26.2)
Females $(n=7)$	439.9 ± 12.8 (428–460)	80.0±1.5 (77–82)	71.7±2.0 (68–74)	63.8±2.3 (59–66)	60.9±3.5 (55–64)	19.5±0.6 (18.5–20.6)	22.4±1.9 (19.2–24.5)

The medial and lateral AP depths were measured in the axial plane along a line perpendicular to the coronal plane and extending anterior from the points where the coronal plane was tangent to the posterior femoral condyles.

- [22] Roth, J. D., Howell, S. M., and Hull, M. L., 2019, "Analysis of Differences in Laxities and Neutral Positions From Native After Kinematically Aligned TKA Using Cruciate Retaining Implants," J. Orthop. Res., 37(2), pp. 358–369.
 [23] Asano, T., Akagi, M., and Nakamura, T., 2005, "The Functional Flexion-
- [23] Asano, T., Akagi, M., and Nakamura, T., 2005, "The Functional Flexion-Extension Axis of the Knee Corresponds to the Surgical Epicondylar Axis: In Vivo Analysis Using a Biplanar Image-Matching Technique," J. Arthroplasty, 20(8), pp. 1060–1067.
- [24] Eckhoff, D. G., Bach, J. M., Spitzer, V. M., Reinig, K. D., Bagur, M. M., Baldini, T. H., and Flannery, N. M., 2005, "Three-Dimensional Mechanics, Kinematics, and Morphology of the Knee Viewed in Virtual Reality," J. Bone Jt. Surg., 87(suppl_2), pp. 71–80.
- [25] Pinskerova, V., Johal, P., Nakagawa, S., Sosna, A., Williams, A., Gedroyc, W., and Freeman, M. A., 2004, "Does the Femur Roll-Back With Flexion?," J. Bone Jt. Surg. Br. Vol., 86-B(6), pp. 925–931.
- [26] Churchill, D. L., Incavo, S. J., Johnson, C. C., and Beynnon, B. D., 1998, "The Transepicondylar Axis Approximates the Optimal Flexion Axis of the Knee," Clin. Orthop. Relat. Res., 356, pp. 111–118.
- [27] Alesi, D., Marcheggiani Muccioli, G. M., Roberti di Sarsina, T., Bontempi, M., Pizza, N., Zinno, R., Di Paolo, S., Zaffagnini, S., and Bragonzoni, L., 2021, "In Vivo Femorotibial Kinematics of Medial-Stabilized Total Knee Arthroplasty

- Correlates to Post-Operative Clinical Outcomes," Knee Surg. Sports Traumatol. Arthrosc., **29**(2), pp. 491–497.
- [28] Elorza, S. P., O'Donnell, E., Delman, C., Howell, S. M., and Hull, M. L., 2023, "Posterior Cruciate Ligament Retention With Medial Ball-in-Socket Conformity Promotes Internal Tibial Rotation and Knee Flexion While Providing High Clinical Outcome Scores," Knee, 43, pp. 153–162.
 [29] Shimmin, A., Martinez-Martos, S., Owens, J., Iorgulescu, A. D., and Banks, S.,
- [29] Shimmin, A., Martinez-Martos, S., Owens, J., Iorgulescu, A. D., and Banks, S., 2015, "Fluoroscopic Motion Study Confirming the Stability of a Medial Pivot Design Total Knee Arthroplasty," Knee, 22(6), pp. 522–526.
- [30] Steinbruck, A., Schroder, C., Woiczinski, M., Fottner, A., Pinskerova, V., Muller, P. E., and Jansson, V., 2016, "Femorotibial Kinematics and Load Patterns After Total Knee Arthroplasty: An In Vitro Comparison of Posterior-Stabilized Versus Medial-Stabilized Design," Clin. Biomech., 33, pp. 42–48.
- [31] Yin, L., Chen, K., Guo, L., Cheng, L., Wang, F., and Yang, L., 2015, "Identifying the Functional Flexion-Extension Axis of the Knee: An in-Vivo Kinematics Study," PLoS One, 10(6), p. e0128877.
- [32] Kornaat, P. R., Koo, S., Andriacchi, T. P., Bloem, J. L., and Gold, G. E., 2006, "Comparison of Quantitative Cartilage Measurements Acquired on Two 3.0T MRI Systems From Different Manufacturers," J. Magn. Reson. Imaging, 23(5), pp. 770–773.